Acta Mechanica Sinica (2014) 30(3):339–350
DOI 10.1007/s10409-014-0018-9

RESEARCH PAPER

Scaling law of resolved-scale isotropic turbulence and its application in large-eddy simulation

Le Fang · Bo Li · Li-Peng Lu

Received: 4 September 2013 / Revised: 4 December 2013 / Accepted: 4 December 2013

Abstract Eddy-damping quasinormal Markovian (EDQNM) theory is employed to calculate the resolved-scale spectrum and transfer spectrum, based on which we investigate the resolved-scale scaling law. Results show that the scaling law of the resolved-scale turbulence, which is affected by several factors, is far from that of the full-scale turbulence and should be corrected. These results are then applied to an existing subgrid model to improve its performance. A series of simulations are performed to verify the necessity of a fixed scaling law in the subgrid modeling.

Keywords Scaling law · Large-eddy simulation · CZZS model

1 Introduction

Kolmogorov introduced the 2/3 scaling law for the second-order structure function in isotropic turbulence, which is usually named K41 theory. As one of the most important basic theories, the scaling law have attracted plenty of researches in the past seventy years. In order to clarify the background of this paper, we would like to briefly present three important directions in the research of the scaling law: (1) Scaling law in inertial range has been always in the center of the turbulence research. In Kolmogorov 1941 (K41) theory the 2/3 scaling law was obtained by the dimensional analysis, however, it was doubted by Landau and Lifshitz [1] and led to researches on the anomalous scaling law. The anomalous scaling law is usually considered to be generated by the intermittency of the small-scale turbulence. Kolmogorov et al. [2, 3] introduced their corrected scaling laws, which have been proved in lots of experiments and numerical simulations. In addition, Benzi et al. [4] introduced the extended scale-similarity (ESS) theory to improve the scaling law at low Reynolds number, which regarded the (anomalous) skewness of velocity increment as a constant. There are also several researchers who doubted the anomalous scaling law. Qian [5, 6] argued that the anomalous scaling law might be a finite Reynolds effect (FRE), while K41 theory should be satisfied at infinite Reynolds number. Barenlatt [7] argued that the relative scaling exponent in ESS theory should not be an anomalous number 0.70 but should remain 2/3. There is still no conclusion on these arguments, and in the modern researches the main trend is still the anomalous scaling law and intermittency. (2) Both K41 theory and anomalous scaling law can be employed only in inertial range of high Reynolds turbulence. These theories are not valid when the two-point distance is close to the dissipation scale or energy-containing scale. In order to investigate the scaling law outside inertial range, one method is to combine the Kolmogorov equation with ESS theory. ESS theory can more or less extend the scaling law, however, it is still not valid for studying the transition between dissipation range and inertial range unless some models are introduced on the skewness [8]. Not considering this transition range and only solving the differ-

The project was supported by the National Natural Science Foundation of China (11202013 and 51136003), the National Basic Research Program of China (2012CB720200), and the Opening fund of State Key Laboratory of Nonlinear Mechanics.

L. Fang (✉)
École Centrale de Pékin, Beihang University,
100191 Beijing, China
The State Key Laboratory of Nonlinear Mechanics,
Chinese Academy of Science, 100190 Beijing, China
e-mail: le.fang@zoho.com

B. Li
Laboratoire de Mécanique des Fluides et d'Acoustique,
Université de Lyon, École centrale de Lyon,
69134 Ecully, France

L.-P. Lu
School of Energy and Power Engineering,
Beihang University, 100191 Beijing, China

ence equations in dissipation range and inertial range seperately can lead to the scaling law of series [9]. There is still no good theoretical result to describe the transition between dissipation range and inertial range, while the most accurate result should be the interpolation equation by Batchelor [10]. Although this equation is semi-empirical, it is in good agreement with the experimental and theoretical results [9, 11, 12]. In addition, the transition between inertial range and energy-containing range depends on the large-scale structures and still lacks investigations. (3) Besides, some researchers focus on the sclaing law in anisotropic turbulence such as the wall-bounded turbulence. Since in this paper we only discuss the isotropic turbulence, we would not talk more about these advances.

The large-eddy simulation (LES) method has been widely employed in the engineering projects. The core problem of LES is the development of the subgrid-scale (SGS) models which denote some physical relationship between scales. In subgrid modeling, the scaling law can be an important tool to describe the multi-scale properties of turbulence [13, 14]. However, it should be emphasized that, in LES we only know the information of the resolved-scale turbulence and can not directly employ the full-scale scaling law.

We have introduced plenty of researches in the paragraphs above, the analysis of the resolved-scale scaling law after filtering is still lacking. Indeed, the necessity of the resolved-scale scaling law for a SGS model is still unclear. This resulted in some confused applications in the existing SGS models. For instance: the original form of the Cui–Zhou–Zhang–Shao (CZZS) model does not fix the resolved-scale scaling law, while in this paper we will show that it is unstable in calculations; one modification of the CZZS model directly used the full-scale scaling law for the resolved part [13], we will point out their great error in this paper; some preliminary analyses were made to support the improved velocity increment (IVI) model by Fang et al. [14], but there was no quantitative result.

In this regard, a comprehensive correction for the resolved-scale scaling law should be necessary, which can provide a more reliable tool for LES. This correction is mainly concerned with three factors: Firstly, the ratio of two-point distance to filter width; Secondly, the LES Reynolds number which can explicitly represent the filter effect (similar to the FRE effect for full-scale turbulence) in the SGS models; Thirdly, the effect of different types of filters. Berland et al. [15] used the eddy-damping quasinormal Markovian (EDQNM) theory to investigate the filter effect on the subgrid stress , but the investigation of the resolved-scale scaling law is still lacking.

We have mentioned in the first paragraph that scholars still have some arguements on the anomalous scaling law. Note that the main point of this paper is neither support nor oppose the anomalous scaling law. We suppose that the correct full-scale scaling law has been obtained (by EDQNM theory for example), which satisfies either K41 law or anomalous law in inertial range. Then we investigate the effect of the filtering operation in LES and the corrections needed. These corrections would be important in LES modeling.

The paper is organized as follows: In the next section, we obtain the resolved-scale energy spectrum and transfer spectrum by using EDQNM theory. Based on these spectra, we analyze the resolved-scale scaling law for the second- and third-order structure functions. In Sect. 3, we employ these results in the subgrid modeling. The CZZS model in different forms will be employed for LES of the free-decay isotropic turbulence to verify the necessity of a fixed correct scaling law in the subgrid modeling. At last, we will further discuss some problems we mentioned in the previous paragraphs.

2 Resolved-scale scaling law

2.1 Energy spectrum and energy transfer spectrum of resolved-scale turbulence

In order to investigate the resolved-scale scaling law, we need the resolved-scale structure functions. Since the resolved-scale structure functions cannot be simply obtained by the full-scale structure functions, we must calculate the resolved-scale energy spectrum and energy transfer spectrum, and then transform them to the resolved-scale second- and third-order structure functions.

There are some simple analytical models for the energy spectrum, such as Pope's model [16] and Pao's model [17]. However, there are no corresponding models for the transfer spectrum. Some statistical models, such as direct interaction approximation (DIA) [18] and test field method (TFM) [19], can provide both energy spectrum and transfer spectrum, but they still have some defects in describing the physical properties of turbulence. The most common analytical model should be EDQNM model [20, 21], which assumes a quasi-normal closure between the second- and fourth-order spectral correlation tensors. In this paper we choose EDQNM theory as the main tool of investigation. The feasibility of this idea could be found in the recent work of Bos et al. [22] and Tchoufag et al. [23].

The resolved energy spectrum can be obtaind by the full-scale spectrum $E(k)$ and the filter kernel $G(k)$

$$E^<(k) = G^2(k)E(k). \tag{1}$$

The resolved transfer spectrum is more complicated. We write $T(k)$ as an integral of the triad interactions $T(k) = \iint \mathrm{d}p\mathrm{d}qT(k,p,q)$, which is a function of $E(k)$ from EDQNM theory

$$T(k,p,q) = \theta_{kpq}\frac{k}{pq}b(k,p,q)E(q)(k^2E(p) - p^2E(k)), \tag{2}$$

where θ_{kpq} and b are functions of wave numbers k, p, and q. When we introduce the filter kernel $G(k)$, the resolved triad

interaction reads

$$T^<(k,p,q) = \theta_{kpq}\frac{k}{pq}b(k,p,q)G^2(q)E(q) \times(k^2G^2(p)E(p) - p^2G^2(k)E(k)), \quad (3)$$

while the resolved transfer spectrum is

$$T^<(k) = \iint \mathrm{d}p\mathrm{d}qT^<(k,p,q). \quad (4)$$

Figure 1 shows the EDQNM results at Taylor-based Reynolds number $Re_\lambda \approx 33\,000$. Both spectra indicate that the wavenumber of filter k_c locates in inertial range. From the energy spectra in Fig. 1a, we find that only the cutoff filter produces a "clean" truncation, while for the other filters there still remains a part of higher-wavenumber energy. However, the resolved-scale transfer spectrum is not simply a truncation of the full-scale one, as could be clearly observed in Fig. 1b. The energy which should dissipate in dissipative range now accumulates around the filter. Therefore, it is reasonable to consider the effect of the filter as reducing the dissipation wavenumber to the wavenumber of filter. In addition, the resolved transfer spectrum of the cutoff filter has a strong interruption around k_c because of the high gradient of the resolved-scale energy spectrum.

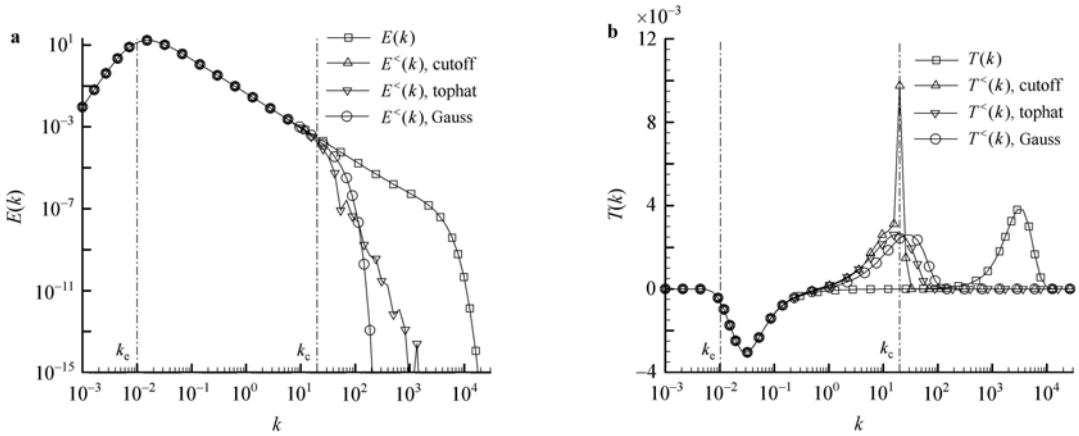

Fig. 1 Non-filtered and filtered spectra from EDQNM theory. Wavenumber of filter $k_c = 20$. Taylor-based Reynolds number $Re_\lambda \approx 33\,000$. LES Reynolds number $Re_\Delta \approx 41$. **a** Energy spectrum; **b** Transfer spectrum

In order to better understand the importance of the filter in LES, we define an "LES" Reynolds number as [17]

$$Re_\Delta = \frac{1}{\sqrt{15}}\left(\frac{k_c}{k_e}\right)^{2/3}, \quad (5)$$

where k_e is the energy-containing wavenumber, and in this case $k_e = 0.01$. Re_Δ should be an important parameter in LES since it denotes the location of the filter compared with energy-containing scale. Although we expect Re_Δ to be implemented in LES, most of the existing SGS models are based on the infinite Reynolds assumption and the effect of Re_Δ can not be explicitly found in these models [24]. This implies that in most existing SGS models the influence of energy-containing information, which can affects both the energy-decaying rate [25] and the spectrum evolution [23], is not explicitely taken into account. In the following parts of this paper we will show that Re_Δ is related with the resolved scaling law, and can then be incorporated into several SGS models.

2.2 Analysis of resolved-scale scaling law

With the resolved-scale energy spectrum and energy transfer spectrum obtained from EDQNM theory, we can calculate the corresponding resolved-scale structure functions with the transform equations derived by Qian [5, 6].

The transform equation between the second-order structure function $D_{\mathrm{II}}(r)$ and the energy spectrum $E(k)$ is [6]

$$D_{\mathrm{II}}(r) = 4\int_0^\infty E(k)\left[\frac{1}{3} + \frac{\cos(kr)}{(kr)^2} - \frac{\sin(kr)}{(kr)^3}\right]\mathrm{d}k. \quad (6)$$

The transform equation between the third-order structure function $D_{\mathrm{III}}(r)$ and the energy transfer spectrum $T(k)$ is [5]

$$D_{\mathrm{III}}(r) = 12r\int_0^\infty T(k)\left[-\frac{\sin(kr)}{(kr)^3} - \frac{3\cos(kr)}{(kr)^4} + \frac{3\sin(kr)}{(kr)^5}\right]\mathrm{d}k. \quad (7)$$

The scaling law of the second- and third-order structure functions can then be obtained by

$$n(2) = \frac{\mathrm{d}D_{\mathrm{II}}(r)}{\mathrm{d}r}\frac{r}{D_{\mathrm{LL}}(r)} \quad (8)$$

and

$$n(3) = \frac{\mathrm{d}D_{\mathrm{III}}(r)}{\mathrm{d}r}\frac{r}{D_{\mathrm{III}}(r)}. \quad (9)$$

Note that Eqs. (6)–(9) are all based on the full-scale turbulence. The corresponding resolved-scale transform equations and scaling law could be simply obtained by replacing

the full-scale quantities with the resolved-scale ones.

Our investigations focus on the effect of the two-point distance r and the LES Reynolds number Re_Δ on the scaling exponents $n(2)$ and $n(3)$. We observe the evolution of the scaling exponents for different values of r and Re_Δ while keeping the other parameters unchanged.

When $Re_\lambda \approx 33\,000$ and $k_c = 20$, the scaling exponents for different r/Δ can be found in Fig. 2. In this case Δ locates in inertial range, and the energy-containing scale is about 1500Δ. Thus, r is in inertial range when $1 \leqslant r/\Delta \ll 1\,500$. The full-scale second-order scaling exponent (the "non-filtered" line) is almost the same as its analytical value 2/3, though there is still a little difference. This difference could be explained either by the anomalous scaling law [2] or by the FRE [9]. Similarly, the full-scale third-order scaling exponent is almost the same as its analytical value 1.

These scaling exponents change after the filter is introduced. Although the values in the large scale (the magnitude of the energy-containing scale) are still the same, in the small scale $r/\Delta < 10$ the resolved scaling exponents are evidently far from their analytical values in the full scale. This phenomenon is caused by the filter, and different filter brings different scaling exponents in this region. For $r = \Delta$, the resolved second-order scaling exponent with the cutoff filter is about 1.79, while with the tophat and Gauss filter it is 1.51 and 1.24, respectively. The resolved third-order scaling exponent with the cutoff filter is about 2.47, which is in agreement with Fang's proposition 2.5 in the IVI model [14], while with the tophat and Gauss filter it is 2.03 and 1.65, respectively. These values are all far from their analytical values in the full scale.

When $Re_\lambda \approx 33\,000$, the scaling exponents with different Re_Δ (by changing k_c) are shown in Figs. 3 and 4 for $r = \Delta$ and $r = 2\Delta$, respectively. These figures are useful since in most of LES applications we set $r = \Delta$ or $r = 2\Delta$. It is found that the scaling exponent is nearly constant in the region $10 < Re_\Delta < 70$. When Re_Δ is very large, both Δ and r locate in dissipative range. Since in LES the filter scale cannot locate in dissipative range, and the LES Reynolds number cannot be large because of the computational cost, it is meaningless to discuss the situation under large LES Rey-

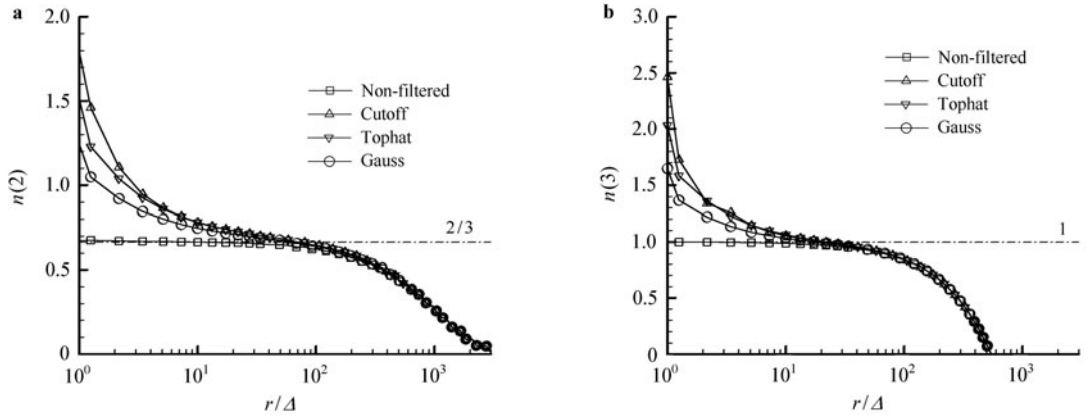

Fig. 2 Scaling exponents from EDQNM theory. Wavenumber of filter $k_c = 20$. Taylor-based Reynolds number $Re_\lambda \approx 33\,000$. LES Reynolds number $Re_\Delta \approx 41$. **a** Scaling exponent of second-order structure function $n(2)$; **b** Scaling exponent of third-order structure function $n(3)$

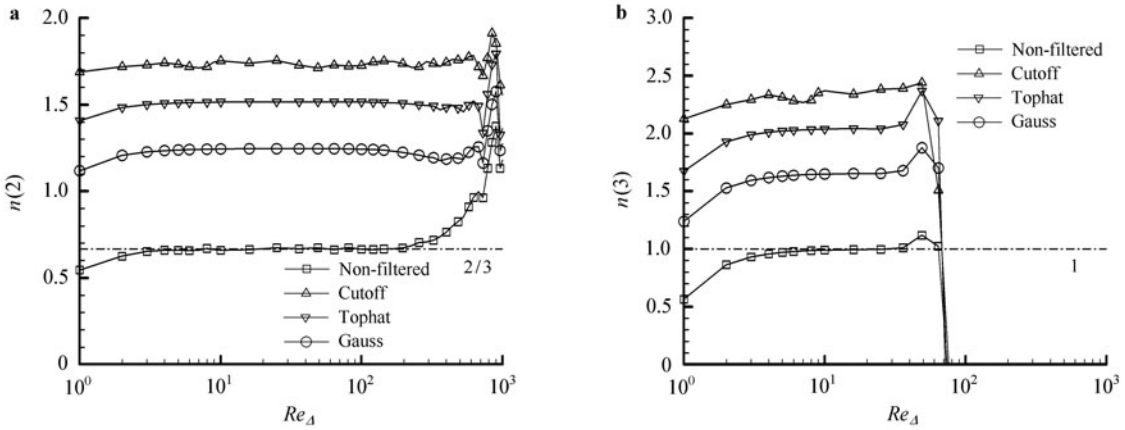

Fig. 3 Scaling exponents from EDQNM theory. Taylor-based Reynolds number $Re_\lambda \approx 33\,000$. Two-point distance $r = \Delta = \pi/k_c$. **a** Scaling exponent of second-order structure function $n(2)$; **b** Scaling exponent of third-order structure function $n(3)$

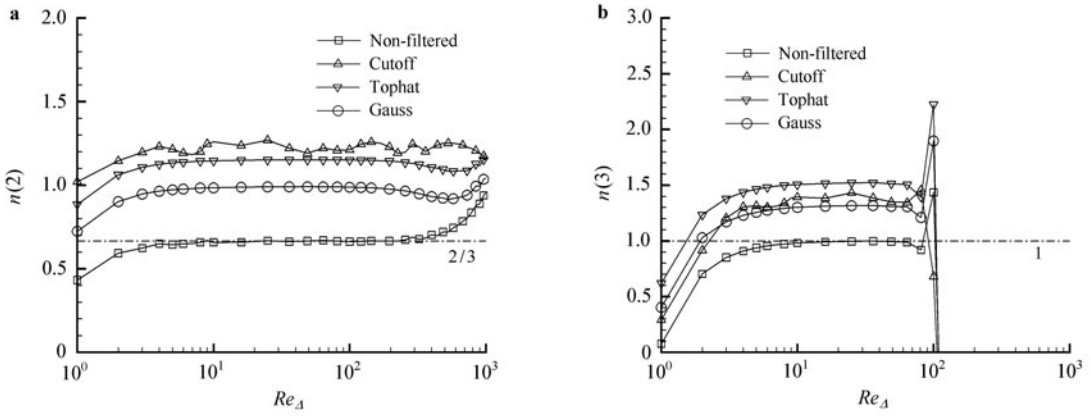

Fig. 4 Scaling exponents from EDQNM theory. Taylor-based Reynolds number $Re_\lambda \approx 33\,000$. Two-point distance $r = 2\Delta = 2\pi/k_c$. **a** Scaling exponent of second-order structure function $n(2)$; **b** Scaling exponent of third-order structure function $n(3)$

nolds number. In contrast, we find that when $Re_\Delta < 10$ the scaling exponents increase with the LES Reynolds number. Thus, we should do the correction on the resolved-scale scaling law in this region. In order to explain the effect of the LES Reynolds number more clearly, we analyze an example as follows. Considering an LES case with 48^3 grids, since the energy-containing scale should not be larger than the size of the computational domain, the ratio of energy containing scale to filter scale cannot be greater than 48, which corresponds to $Re_\Delta \approx 3.4$. The correct value of the scalings can then be found from Figs. 3 and 4 for this LES case, with Re_Δ taken into account.

2.3 Analytical expression of the resolved-scale scaling law

Results in the previous subsection reveal the effect of different parameters on the resolved-scale scaling law, such as the type of filter, the ratio of two-point distance to filter width r/Δ and the LES Reynolds number Re_Δ. In practical LES applications, the scaling exponent may change from time to time. In order to obtain a more precise value of the scaling exponent under different conditions, we need an analytical expression considering the parameters listed above. We assume a simple model for the resolved-scale energy spectrum as follows

$$E^<(k) = \begin{cases} Ak^{-5/3}, & k_e < k < k_c, \\ 0, & \text{otherwise.} \end{cases} \tag{10}$$

With Eqs. (6) and (8) we can calculate the resolved second-order scaling exponent as

$$n(2) = \frac{3\displaystyle\int_{x_e}^{x_c} x^{-5/3}\left(-\frac{\sin x}{3x} - \frac{\cos x}{x^2} + \frac{\sin x}{x^3}\right)\mathrm{d}x}{\displaystyle\int_{x_e}^{x_c} x^{-5/3}\left(\frac{1}{3} + \frac{\cos x}{x^2} - \frac{\sin x}{x^3}\right)\mathrm{d}x}, \tag{11}$$

where $x_e = k_e r$, $x_c = k_c r$.

Note that $n(2)$ is a function of r/L and r/Δ. L is the integral length scale which represents the length scale of large eddies in the flow. Thus, we consider the effect of the LES Reynolds number Re_Δ in this analytical expression of the resolved-scale scaling law.

This analytical expression could be rewritten as

$$n(2) = \frac{\mathcal{F}(x_c) - \mathcal{F}(x_e)}{\mathcal{H}(x_c) - \mathcal{H}(x_e)}, \tag{12}$$

in which

$$\begin{aligned} \mathcal{F}(x) &= -\frac{9}{11}\frac{\sin x}{x^{11/3}} + \frac{9}{11}\frac{\cos x}{x^{8/3}} + \frac{6}{55}\frac{\sin x}{x^{5/3}} \\ &\quad + \frac{9}{55}\frac{\cos x}{x^{2/3}} - \frac{9}{220}\mathcal{T}(x), \\ \mathcal{H}(x) &= -\frac{1}{2x^{2/3}} + \frac{3}{11}\frac{\sin x}{x^{11/3}} - \frac{3}{11}\frac{\cos x}{x^{8/3}} \\ &\quad + \frac{9}{55}\frac{\sin x}{x^{5/3}} + \frac{27}{110}\frac{\cos x}{x^{2/3}} - \frac{27}{440}\mathcal{T}(x), \\ \mathcal{T}(x) &= (1 + \sqrt{3}\iota)\Gamma(1/3, \iota x) \\ &\quad + (1 - \sqrt{3}\iota)\Gamma(1/3, -\iota x), \end{aligned} \tag{13}$$

where $\iota = \sqrt{-1}$. $\Gamma(s, x)$ is the incomplete Gamma function $\Gamma(s, x) = \displaystyle\int_x^\infty t^{s-1}\mathrm{e}^{-t}\mathrm{d}t$.

Considering the fact that the flows in engineering applications generally have a high Reynolds number, it is reasonable to further simplify the analytical expression of $n(2)$ with the infinite Reynolds assumption $k_e = 0$

$$\begin{aligned} \mathcal{F}(x) &= \frac{9}{11}\frac{(-1)^m}{(m\pi)^{8/3}} + \frac{9}{55}\frac{(-1)^m}{(m\pi)^{2/3}} - \frac{9}{110}\mathcal{T}(m\pi), \\ \mathcal{H}(x) &= \frac{27}{110}\frac{(-1)^m}{(m\pi)^{2/3}} - \frac{1}{2(m\pi)^{5/3}} \\ &\quad - \frac{3}{11}\frac{(-1)^m}{(m\pi)^{8/3}} - \frac{27}{220}\mathcal{T}(m\pi), \end{aligned} \tag{14}$$

where $m = r/\Delta \in \mathbb{N}^*$. In LES we often fix the ratio of two-point distance to filter width r/Δ as an integer. The corresponding scaling exponents are shown in Table 1. In practical LES applications with high Reynolds number, we may approximately use these values.

Table 1 Scaling exponents from Eq. (12) with $k_e = 0$

r/Δ	1	2	3	4	5
$n(2)$	1.742 7	1.246 7	0.999 6	0.932 7	0.877 5
r/Δ	6	7	8	9	10
$n(2)$	0.850 5	0.825 9	0.811 0	0.796 8	0.787 2

Unfortunately, it is difficult to obtain an analytical expression of the resolved third-order scaling exponent $n(3)$, since we have no simple model for the energy transfer spectrum $T(k)$, not to mention the resolved one [23]. When $n(3)$ is needed in practical LES applications, we could refer to Figs. 2b, 3b, and 4b for an approximate value.

3 Applications of resolved-scale scaling law in LES

An appropriate choice of subgrid model would affect the resolved-scale behavior [26–28] as well as the time correlation statistics [29]. Besides, in the simulation of heavy particles, it is also found that the choice of subgrid model is related to the computational accuracy of particles [30–34]. The aim of the research on resolved-scale scaling law is to provide a better tool for the subgrid modeling in LES. In this section, we will elaborate its application to the CZZS model [13], a typical SGS model based on the structure functions.

The CZZS model is derived from the resolved-scale Kolmogorov equation. With the eddy-viscosity assumption, its original form is

$$\nu_t = \frac{-5D^<_{III}(r)}{8\langle S^<_{ij}S^<_{ij}\rangle r - 30\mathrm{d}D^<_{II}(r)/\mathrm{d}r}. \tag{15}$$

We can further simplify the model with the resolved-scale scaling law by introducing Eq. (8). The modified form reads

$$\nu_t = \frac{-5D^<_{III}(r)}{8\langle S^<_{ij}S^<_{ij}\rangle r - 30n(2)D^<_{II}(r)/r}, \tag{16}$$

where $n(2)$ is the scaling exponent of the resolved-scale second-order structure function.

It should be emphasized that both forms of the CZZS model contain the information of the resolved-scale scaling law. For the modified form (16), the information is involved explicitely in the resolved second-order scaling exponent $n(2)$. The value of $n(2)$ could be determined either by the figures or by its analytical expression derived in the previous section. In contrast, the information is involved implicitely in the original form (15), which could be clearly observed if we rewrite the model as

$$\nu_t = \frac{-5D^<_{III}(r)}{8\langle S^<_{ij}S^<_{ij}\rangle r - 30\left(\frac{\mathrm{d}D_{II}(r)}{\mathrm{d}r}\frac{r}{D_{II}(r)}\right)D^<_{II}(r)/r}. \tag{17}$$

The original form (15) is equivalent to the modified form (16) with $n(2)$ determined dynamically by its definition. In other words, the resolved-scale scaling law that we utilize in the original form of the CZZS model is determined dynamically, while in the modified form we fix a resolved-scale scaling law which is derived in the previous section. In the following simulations, the results will show their difference and reveal the importance of fixing a correct scaling law.

We employ the CZZS model in different forms for LES of the homogeneous isotropic turbulence. Our LES cases correspond to the free-decay turbulence at high Reynolds number by setting the molecular viscosity to a very small value. The discussion about free-decay turbulence and forcing turbulence can be found in Sect. 4.3. These simulations are performed on 32^3, 48^3, 64^3, 96^3, 128^3, and 256^3 grids, respectively. Only the results of 32^3, 64^3, and 128^3 are presented, since they show the same variation tendency with the resolution. The spectral method is applied in these cases. The initial field is generated by using Rogallo's method [35] with randomly distributed velocity phases. Some computational parameters are showed in Table 2. In order to assess the performance of the SGS model, the spectra will be taken to compare with the ones computed from the Métais–Lesieur model [36]. The normalized time denoted as t^* in all figures is based on a characteristic time τ of the free-decay turbulence defined as [37]

$$\tau = \sqrt{\frac{3}{2}}\frac{k_t}{\varepsilon}, \tag{18}$$

where k_t and ε correspond to the turbulent kinetic energy and dissipation rate of the initial field, respectively.

Table 2 Parameters implemented in numerical simulations

Molecular viscosity ν	$10^{-9}\mathrm{m}^2/\mathrm{s}$
Time step Δt	0.000 1 s
Length of computational domain H	2π

3.1 CZZS model with dynamically-determined scaling law

As discussed above, the original form of the CZZS model utilizes a dynamically-determined scaling law. It is reasonable to consider that the resolution has an effect on the performance of the model.

Figures 5a, 6a, and 7a show the spectra computed from the Métais–Lesieur model. The spectra are in good agreement with the $-5/3$ power law of inertial range. In these cases the Métais–Lesieur model performs well, which makes it possible to regard it as a reference to assess the performance of the CZZS model.

For the cases of 32^3 and 64^3 shown in Figs. 5b and 6b, the CZZS model performs well in the early stage. However, the energy gradually accumulates around the cutoff wavenumber and the computations tend to diverge. A too small eddy viscosity computed from the CZZS model may account for these results. As for the case of 128^3, a similar phenomenon could be observed, though the result is acceptable. Theoretically, we need an eddy viscosity decreasing

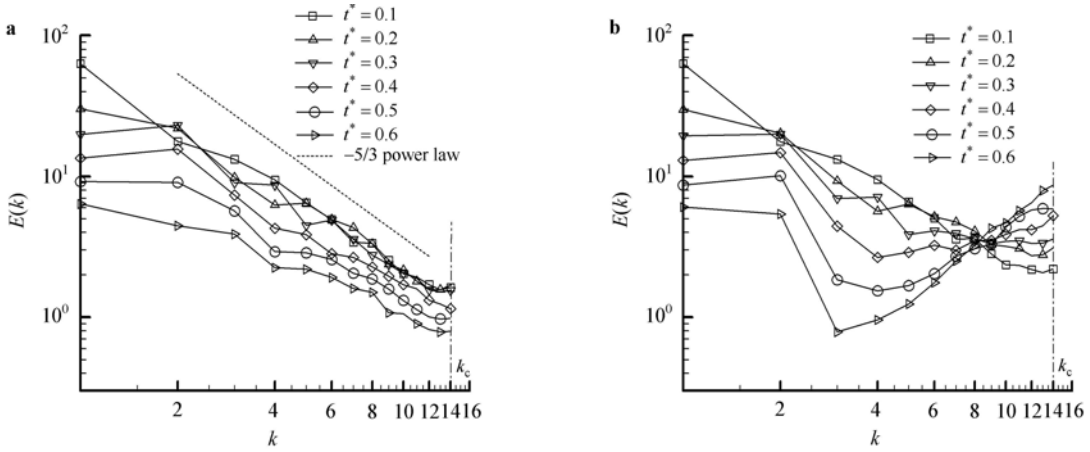

Fig. 5 Comparison of spectra in free-decay isotropic turbulence, 32^3 LES runs. **a** Métais–Lesieur model; **b** CZZS model with dynamically-determined scaling law

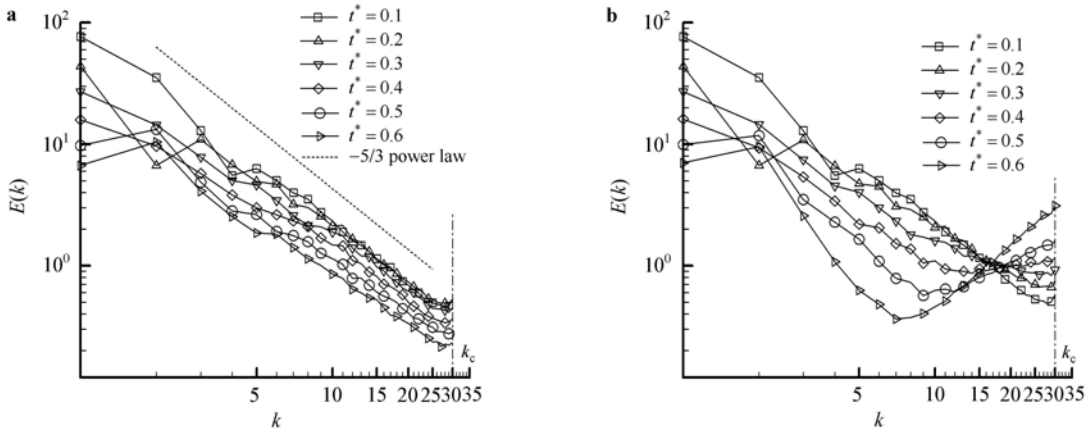

Fig. 6 Comparison of spectra in free-decay isotropic turbulence, 64^3 LES runs. **a** Métais–Lesieur model; **b** CZZS model with dynamically-determined scaling law

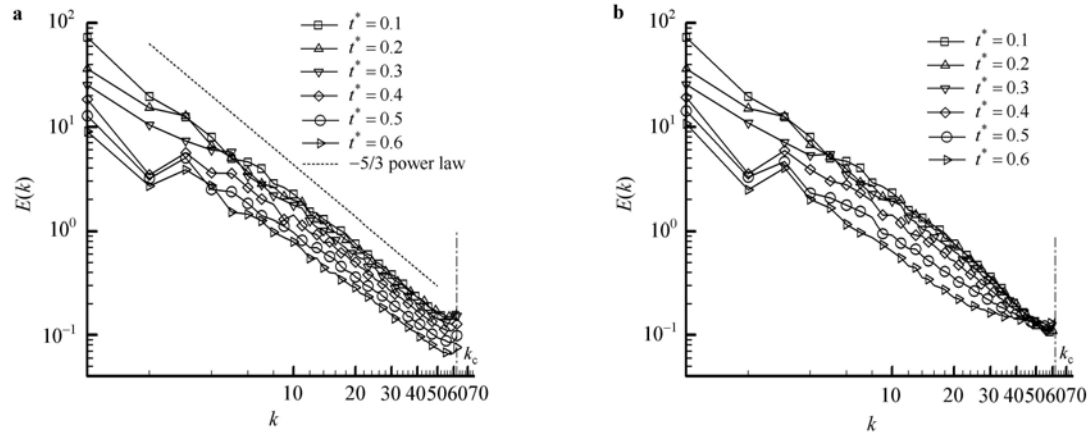

Fig. 7 Comparison of spectra in free-decay isotropic turbulence, 128^3 LES runs. **a** Métais–Lesieur model; **b** CZZS model with dynamically-determined scaling law

with time for the free-decay turbulence, whereas the eddy viscosity computed from the CZZS model decreases more rapidly than we expect when the scaling law is dynamically determined. The CZZS model does not show enough ability of self-adjustment and therefore becomes unstable.

It should be emphasized that this instability may be nu-

merical, not physical. From the comparison between different resolutions, we observe a better result with the increase of resolution, which makes it possible to associate these unsatisfactory results with low resolution. Therefore from the current test case we can conclude that, a dynamically-determined scaling law in the CZZS model probably leads to numerical instability.

3.2 CZZS model with fixed full-scale scaling law

In the original paper of CZZS model, the simplified model was obtained by assuming the full-scale 2/3 scaling law [13]. In this paper, we have shown that the resolved-scale scaling law is by no means the same as the full-scale scaling law, and the resolved-scale scaling exponent is far from the full-scale analytical value. The full-scale 2/3 scaling law is a fixed scaling law but not the correct one in LES. The result of simulation in Fig. 8 further supports our point of view. The energy accumulating around the cutoff wavenumber has even the same magnitude as the energy contained in energy containing range, which could be explained by a too weak dissipation in the subgrid scale. Finally all the test cases in Fig. 8 diverge due to this lack of dissipation.

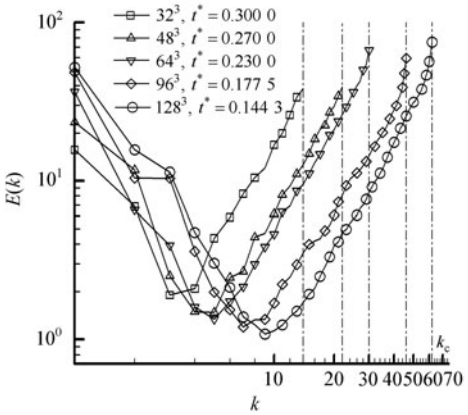

Fig. 8 Near-diverged spectra computed from CZZS model with $n(2) = 2/3$

3.3 CZZS model with fixed resolved-scale scaling law

In Sects. 3.1 and 3.2 it is shown that CZZS model with neither a dynamically-determined scaling law nor a fixed full-scale scaling law could obtain satisfactory energy spectra. In this subsection, we introduce the fixed resolved-scale scaling law derived in the previous section into the CZZS model and perform the same simulations as above. The results will show the significance of our research.

In the previous section, we obtain a value of $n(2)$ for $r = \Delta$, 1.74, under the infinite Reynolds assumption. Since our cases have a high Reynolds number, it is reasonable to directly adopt this value as $n(2)$. The results are showed in Figs. 9–11. Comparing Figs. 5a, 6a, and 7a, we can conclude that, for most of the parts in the spectra, the difference be-

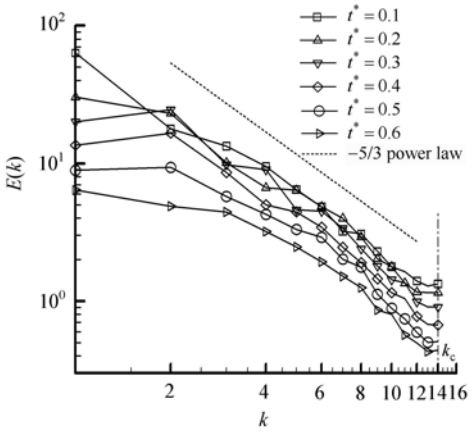

Fig. 9 Energy spectra in free-decay isotropic turbulence, 32^3 LES runs. CZZS model with fixed resolved-scale scaling law, $n(2) = 1.74$

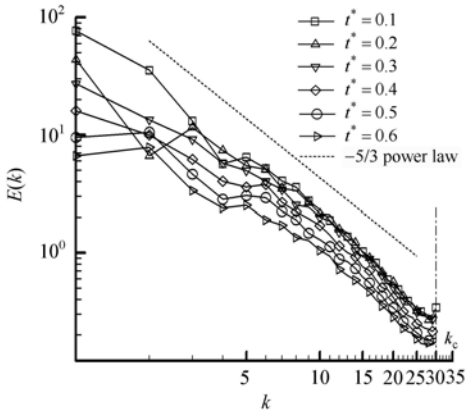

Fig. 10 Energy spectra in free-decay isotropic turbulence, 64^3 LES runs. CZZS model with fixed resolved-scale scaling law, $n(2) = 1.74$

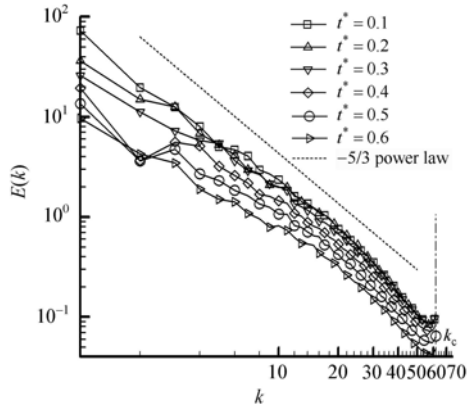

Fig. 11 Energy spectra in free-decay isotropic turbulence, 128^3 LES runs. CZZS model with fixed resolved-scale scaling law, $n(2) = 1.74$

tween CZZS model and Métais–Lesieur model is negligible. The $-5/3$ power law of inertial range behavior can be clearly observed. The only difference could be found around the wavenumber of filter, where CZZS model imports a slightly stronger dissipation and makes the spectra droop. This phenomenon might be explained by the "cusp" treatment on the spectral eddy viscosity in LES cases, which affects the accuracy near the wavenumber of filter, yet is sometimes too sensitive to the local slope of spectra [37, 38].

There still remains a question to answer: Why do we need to fix the scaling law to obtain a satisfactory result? We argue that a well-performed SGS model should focus on two physical behaviors: First, a proper dissipation, which could represent the strong dissipative effect at small scales, is quite important for the numerical stability; second, the multi-scale properties of turbulence, i.e., the interaction between resolved and subgrid scale, usually represent some self-similarity behaviors in inertial subrange. In practical LES applications, this multi-scale interaction involved in the SGS model could be fixed or computed dynamically. A fixed scaling law is then argued to be equivalent to a fixed multi-scale interaction. In contrast, a dynamically-determined multi-scale interaction employed in CZZS model may lead to instability.

4 Discussion

4.1 Applications of scaling law in other SGS models

The scaling law is a tool to describe the multi-scale properties of turbulence, which makes it possible to be useful in the SGS models. There are other potential applications besides the CZZS model.

(1) IVI model. Brun et al. [39] introduced a velocity increment (VI) model based on the same tensor properties of the subgrid stresses tensor and the second-order VI tensor. Fang et al. [14] improved the VI model by employing the Kolmogorov equation for the filtered quantities (KEF) to correct its near-wall behavior and to make it predict well both forward and backward energy transfer. The coefficient of the improved velocity increment (IVI) model reads

$$C_{\mathrm{f}} = \frac{2D^{<}_{\mathrm{III}}(r)}{4r\dfrac{\mathrm{d}D^{<}_{\mathrm{III}}(\xi)}{\mathrm{d}\xi}\Big|_{\xi=r} - 4D^{<}_{\mathrm{III}}(r) - D^{<}_{\mathrm{III}}(2r)}. \tag{19}$$

Similar to the CZZS model, there exists a derivative of the resolved structure function. This model could be simplified by introducing the resolved third-order scaling exponent

$$C_{\mathrm{f}} = \frac{2D^{<}_{\mathrm{III}}(r)}{4(n(3)-1)D^{<}_{\mathrm{III}}(r) - D^{<}_{\mathrm{III}}(2r)}. \tag{20}$$

From direct numerical simulation (DNS) results of channel flow Fang proposed approximately $n(3) = 2.5$, which was already discussed in previous sections of the present paper. From Figs. 2b, 3b, and 4b we are readily able to correct this resolved scaling law in IVI model.

(2) Pumir's SPH model. In the LES of smoothed particle hydrodynamics (SPH), Pumir and Shraiman proposed a time-revesable eddy viscosity SGS model [40]. A key step in the formulation was based on the resolved-scale second-order scaling law, but the authors used the $2/3$ full-scale scaling law (see Eq. (13) of Ref. [40]). Similar to the discussion of CZZS model, this SPH model should also be corrected by employing the resolved scaling law, by considering the two-point distance, the LES Reynolds number and the filter effect.

4.2 ESS theory of resolved-scale turbulence

In practice, we sometimes use the relative scaling law instead of the absolute one [13, 41]. In this subsection we examine the relative scaling law (ESS theory) in the resolved-scale turbulence. The relative scaling exponent is defined by using the skewness of velocity increment

$$S_k(r) = \frac{D_{\mathrm{III}}(r)}{(D_{\mathrm{II}}(r))^{3/2}}, \qquad S^{<}_k(r) = \frac{D^{<}_{\mathrm{III}}(r)}{(D^{<}_{\mathrm{II}}(r))^{3/2}}. \tag{21}$$

In ESS theory, the skewness is constant in a quite large region. However, the possibility of extending this theory to the resolved-scale skewness still needs investigations. Since ESS theory is a function of the two-point distance r, here we only need to fix Re_{Δ} and observe the effect of r. Similar to the previous section, the spectra are obtained by using EDQNM theory. When $Re_{\lambda} \approx 33\,000$ and $k_{\mathrm{c}} = 20$, the skewness of velocity increment can be found in Fig. 12a. In the full-scale turbulence, the skewness is almost constant in inertial range $1 < r/\Delta < 100$. However, in the resolved-scale turbulence, the skewness is not constant around the filter size ($r/\Delta \sim 1$), and it is close to the full-scale skewness only in a small region $r/\Delta \approx 100$. Results show that, the applicable range of ESS theory is reduced in the resolved-scale turbulence, and the resolved-scale skewness should be corrected in the SGS models.

When intermittency is considered, ESS theory is $D_{\mathrm{II}}(r) \propto D_{\mathrm{III}}(r)^{\zeta(2)}$, where $\zeta(2)$ is about 0.7. Similarly, we can define the "intermittent skewness" of velocity increment

$$S^{i}_k(r) = \frac{D_{\mathrm{III}}(r)}{(D_{\mathrm{II}}(r))^{1/\zeta(2)}}, \qquad S^{i<}_k(r) = \frac{D^{<}_{\mathrm{III}}(r)}{(D^{<}_{\mathrm{II}}(r))^{1/\zeta(2)}}. \tag{22}$$

It leads to the values shown in Fig. 12b. The full-scale skewness is no longer constant, but after filtering there is a region $10 < r/\Delta < 100$ in which the skewness is approximately constant. This result is in agreement with the viewpoint of the scholars who supported K41 theory [6, 7] and argued that both absolute and relative scaling laws are caused by FRE. We would like to mention that this preliminary result depends on the robustness of EDQNM calculation and will be further investigated in the future by comparing numerical and experimental results.

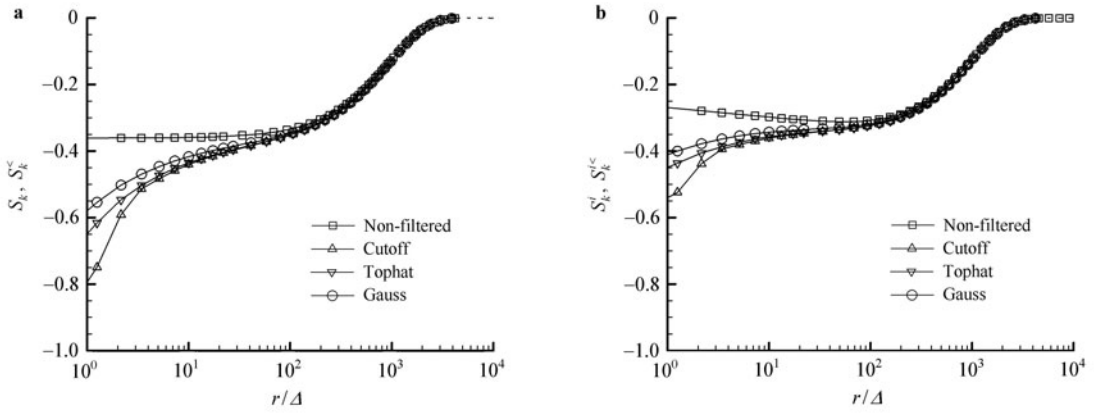

Fig. 12 Skewness of velocity increment from EDQNM theory. Wavenumber of filter $k_c = 20$. Taylor-based Reynolds number $Re_\lambda \approx 33\,000$. LES Reynolds number $Re_\Delta \approx 41$. **a** Intermittency is not considered; **b** Intermittency is considered

4.3 Energy budget of free-decay turbulence and forcing turbulence for CZZS model

We have simulated the free-decay turbulence here by applying the CZZS model. Indeed, if we review the derivation of the CZZS model, it can be found that the model is based on the stationary assumption of small-scale structures, and the temporal term has been neglected. A question then arises: Can the CZZS model be appropriate for simulating the free-decay turbulence, which is definitively not statistically stationary?

In order to clarify this question, a corresponding energy budget should be convincing. The CZZS model is based on the filtered Kolmogorov equation by neglecting several terms

$$D^<_{\mathrm{III}} - 6T_{\mathrm{I,II}} + \frac{4}{5}\varepsilon_{\mathrm{f}}\xi = 0, \tag{23}$$

where the terms on the left hand side are the resolved-scale third-order structure function, the non-linear interactions and the subgrid dissipation, respectively. Here we use ξ to represent the two-point distance. The neglected temporal term is the local integration of $\mathrm{d}D^<_{\mathrm{II}}/\mathrm{d}t$. The application of the CZZS model requires that the error, defined as

$$T^{\mathrm{error}} = D^<_{\mathrm{III}} - 6T_{\mathrm{I,II}} + \frac{4}{5}\varepsilon_{\mathrm{f}}\xi \tag{24}$$

should be negligible. We then perform an a priori test in two DNS databases, which are free-decay turbulence and forcing turbulence, respectively. The instantaneous Reynolds number of free-decay turbulence is $Re_\lambda = 50$, while it is $Re_\lambda = 70$ for the forcing one. In the test, the filter size is fixed as $\Delta = 8h$, which is about 15.2η in the free-decay turbulence and 26.3η in the forcing turbulence. The energy budget of the two-point energy transfer with different two-point distances is shown in Fig. 13. It can be found that in both cases, the error term is small and negligible in the region where the two-point distance $\xi \simeq \Delta$. This supports the current applications of using the CZZS model in free-decay turbulence. In fact, according to our previous analysis, when both the filter size and the two-point distance are in inertial range, the temporal derivation $\mathrm{d}D^<_{\mathrm{II}}/\mathrm{d}t$ is always negligible as compared to other terms.

We would also like to explain the reason why choose the free-decay turbulence in the present paper instead of the forcing one. In the free-decaying process, the Reynolds number is not constant, which requires the dynamic behavior of the SGS model. In contrast, the forcing turbulence corresponds to statistically constant Reynolds number. Therefore, a free-decay test case should be more convincing to verify the current model improvement.

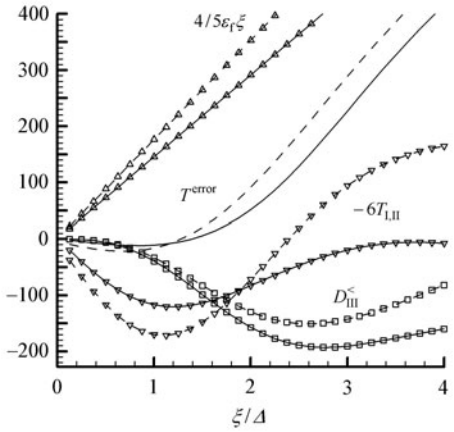

Fig. 13 Exact two-point energy transfer budget in homogeneous isotropic turbulence. Filter size $\Delta = 8h$. Solid line: Free-decay turbulence; Dashed line: Forcing turbulence

5 Conclusion

The spirit of LES is to seperate a velocity field into multiple scales and then to formulate SGS models based on their multi-scale similarity. For SGS models in physical space, this multi-scale similarity is usually represented by the scaling law of velocity structure functions. However, this was usually misused in SGS models, where the full-scale scaling law should be replaced by the resolved-scale scaling law. In

the present paper we investigate the behavior of the resolved-scale scaling law from an EDQNM calculation. Several factors which are important for this scaling law are considered as follows.

(1) Ratio of the two-point distance to the filter size r/Δ. This is similar to the function of r/η in traditional investigations on full-scale scaling laws where the filter size could be approximately regarded as an "enlarged dissipative scale". One corresponding phenomenon is that when a filter is employed, the inertial range observed from scaling laws becomes narrower (see Figs. 2 and 12, where the plateau ranges are narrower with filters). This is similar to the FRE but the mechanism is different. The narrower inertial range leads to a cusp phenomenon near $r \sim \Delta$, which results in a necessary correction in LES applications. For instance, the traditional value $2/3$ on the full-scale second-order structure function shoule be replaced by about 1.79 in the resolved case with a cut-off filter, while for the third-order structure function the scaling law should be approximately 2.47 instead of 1.

(2) "LES" Reynolds number Re_Δ. Inspired from the FRE studies, we propose this concept by considering the filter size as the "dissipative scale in LES" since the dissipative information is lost. This "LES" Reynolds number describes the ratio of energy-containing scale to the filter size, and therefore includes the energy-containing information. Compared to the classical SGS models such as Chollet [42], importing the concept of Re_Δ would allow detailed description of the resolved field and avoid the sensitivity of the energy truncation near filter wave number. It is found that the scaling laws vary with different Re_Δ and could be considered in SGS modeling to take account of the energy-containing information.

(3) Type of filter. In the present paper we disucss three typical filters (cutoff, tophat and Gaussian) and show their influence on the resolved scaling laws. In addition, an analytical model on the resolved-scale second-order scaling law is introduced to consider the influence of r/Δ and Re_Δ.

These results are then employed in SGS models. The CZZS model is taken as an example to simulate the free-decay homogeneous isotropic turbulence at high Reynolds number, and its performance is assessed by referring to the Métais–Lesieur model. Results show that the application of the $2/3$ full-scale scaling law in LES is essentially wrong and should be corrected. The CZZS model with the fixed resolved-scale scaling law derived in the present paper performs well, and the $-5/3$ power law behavior in inertial range could be clearly observed from the spectra. In contrast, when employed with a dynamically-determined scaling law, the CZZS model becomes unstable and yields unsatisfactory results. This phenomenon might be explained by the instability caused by the dynamically determined multi-scale interaction involved in SGS models.

References

1 Landau, L., Lifshits, E.: Fluid Mechanics. Pergmon Press, London (1963)
2 Kolmogorov, A.N.: A refinement of previous hypotheses concerning the local structure of turbulence. Journal of Fluid Mechanics **13**, 82–85 (1962)
3 She, Z.S., Leveque, E.: Universal scaling law in fully developed turbulence. Physics Review Letters **72**, 336 (1994)
4 Benzi, R., Ciliberto, S., Baudet, C., et al.: On the scaling of three-dimensional homogeneous and isotropic turbulence. Physica D **80**, 385–398 (1995)
5 Qian, J.: Inertial range and the finite reynolds number effect of turbulence. Physical Review E **55**, 337–342 (1997)
6 Qian, J.: Normal and anomalous scaling of turbulence. Physical Review E **58**, 7325–7329 (1998)
7 Barenblatt, G., Chorin, A., Prostokishin, V.: Comment on the paper on the scaling of three-dimensional homogeneous and isotropic turbulence, Benzi et al. eds. Physica D **127**, 105–110 (1999)
8 Tatarskii, V.I.: Use of the 4/5 Kolmogorov equation for describing some characteristics of fully developed turbulence. Physics of Fluids **17**, 035110 (2005)
9 Fang, L., Bos, W., Zhou, X., et al.: Corrections to the scaling of the second-order structure function in isotropic turbulence. Acta Mechanica Sinica **26**, 151–157 (2010)
10 Batchelor, G.K.: Pressure fluctuations in isotropic turbulence. Proc. Cambridge Philos. Soc. **47**, 359–374 (1951)
11 Lohse, D., Muller-Groeling, A.: Bottleneck effects in turbulence: scaling phenomena in r versus p space. Physical Review Letters **74**, 1747–1750 (1995)
12 Meneveau, C.: Transition between viscous and inertial-range scaling of turbulence structure functions. Physical Review E **54**, 3657–3663 (1996)
13 Cui, G., Zhou, H., Zhang, Z., et al.: A new dynamic subgrid eddy viscosity model with application to turbulent channel flow. Physics of Fluids **16**, 2835–2842 (2004)
14 Fang, L., Shao, L., Bertoglio, J., et al.: An improved velocity increment model based on Kolmogorov equation of filtered velocity. Physics of Fluids **21**, 065108 (2009)
15 Berland, J., Bogey, C., Bailly, C.: Investigation using statistical closure theory of the influence of the filter shape on scale separation in large-eddy simulation. Journal of Turbulence **9**, N21 (2008)
16 Pope, S.: Turbulent Flows. Cambridge University Press, Cambridge (2000)
17 Hinze, J.O.: Turbulence. (2nd edn.) McGraw-Hill, New York (1975)
18 Kraichnan, R.: The structure of isotropic turbulence at very high Reynolds numbers. Journal of Fluid Mechanics **5**, 497–543 (1959)
19 Edwards, S.: The statistical dynamics of homogeneous turbulence. Journal of Fluid Mechanics **18**, 239–273 (1964)
20 Orszag, S.A.: Lectures on the statistical theory of turbulence. Flow Research Incorporated (1974)
21 Lesieur, M.: Turbulence in Fluids. Kluwer Academic, Dordrecht (1997)
22 Bos, W., Chevillard, L., Scott, J., et al.: Reynolds number effects on the velocity increment skewness in isotropic turbulence. Physics of Fluids **24**, 015108 (2012)

23 Tchoufag, J., Sagaut, P., Cambon, C.: Spectral approach to finnite Reynolds number effects on Kolmogorov's 4/5 law in isotropic turbulence. Physics of Fluids **24**, 015107 (2012)
24 Sagaut, P.: Large Eddy Simulation for Imcompressible Flows. Springer, New York (2006)
25 Touil, H., Bertoglio, J., Shao, L.: The decay of turbulence in a bounded domain. Journal of Turbulence **3**, 49 (2002)
26 Fang, L., Shao, L., Bertoglio, J., et al.: The rapid-slow decomposition of the subgrid flux in inhomogeneous scalar turbulence. Journal of Turbulence **12**, 1–23 (2011)
27 Cui, G., Xu, C., Fang, L., et al.: A new subgrid eddy-viscosity model for large-eddy simulation of anisotropic turbulence. Journal of Fluid Mechanics **582**, 377–397 (2007)
28 Fang, L.: A new dynamic formula for determining the coefficient of smagorinsky model. Theoretical and Applied Mechanics Letters **1**, 032002 (2011)
29 He, G., Rubinstein, R., Wang, L.: Effects of subgrid-scale modeling on time correlations in large eddy simulation. Physics of Fluids **14**, 2186–2193 (2002)
30 Vinkovic, I., Aguirre, C., Simoens, S., et al.: Large eddy simulation of droplet dispersion for inhomogeneous turbulent wall flow. International Journal of Multiphase Flow **32**, 344–364 (2006)
31 Yang, Y., He, G., Wang, L.: Effects of subgrid-scale modeling on lagrangian statistics in large-eddy simulation. Journal of Turbulence **9**, 1–24 (2008)
32 Jin, G., He, G., Wang, L.: Large-eddy simulation of turbulent-collision of heavy particles in isotropic turbulence. Physics of Fluids **22**, 055106 (2010)
33 Jin, G., He, G., Wang, L., et al.: Subgrid scale fluid velocity time scales seen by inertial particles in large eddy simulation of particle-laden turbulence. International Journal Multiphase Flow **36**, 432–437 (2010)
34 Jin, G., He, G.: A nonlinear model for the subgrid timescale experienced by heavy particles in large eddy simulation of isotropic turbulence with a stochastic differential equation. New Journal of Physics **15**, 035011 (2013)
35 Rogallo, R.: Numerical experiments in homogeneous turbulence. NASA TM 81315 (1981)
36 Métais, O., Lesieur, M.: Spectral large-eddy simulation of isotropic and stably stratified turbulence. Journal of Fluid Mechanics **239**, 157–194 (1992)
37 Fang, L., Bos., W., Shao, L., et al.: Time-reversibility of Navier-Stokes turbulence and its implication for subgrid scale models. Journal of Turbulence **13**, 1–14 (2012)
38 Berland, J., Bogey, C., Bailly, C.: A study of differentiation error in large-eddy simulations based on the EDQNM theory. Journal of Computational Physics **227**, 8314–8340 (2008)
39 Brun, C., Friedrich, R., da Silva, C.: A non-linear SGS model based on the spatial velocity increment. Theoretical and Computational Fluid Dynamics **20**, 1–21 (2006)
40 Pumir, A., Shraiman, B.: Lagrangian particle approach to large eddy simulations of hydrodynamic turbulence. Journal of Statistical Physics **113**, 693–700 (2003)
41 Fang, L., Boudet, J., Shao, L.: Les échanges inter-echelles en simulation des grandes échelles. 18^e Congrés Français de Mécanique (2007) (in French)
42 Chollet, J., Lesieur, M.: Parametrization of small scales of three-dimensional isotropic turbulence utilizing spectral closures. Journal of the Atmospheric Sciences **38**, 2747–2757 (1981)